The use of a star-shaped trifunctional acyl chloride for the preparation of polyamide thin film composite membranes

Evelien Maaskant[a], Wouter Vogel[b,c], Theo J. Dingemans[d], Nieck E. Benes[a,*]

[a] *Films in Fluids Group - Membrane Science and Technology cluster, Faculty of Science and Technology, MESA+ Institute for Nanotechnology, University of Twente, P.O. Box 217, 7500 AE Enschede, The Netherlands*
[b] *Faculty of Aerospace Engineering, Delft University of Technology, Kluyverweg 1, Delft, Netherlands*
[c] *DPI, P.O. Box 902, 5600 AX Eindhoven, The Netherlands*
[d] *Applied Physical Sciences, University of North Carolina at Chapel Hill, 121 South Rd, NC, United States*

Abstract

A star-shaped trifunctional acyl chloride bearing ether linkages was synthesized as an alternative to the commonly used trimesoyl chloride (TMC) in the preparation of polyamide thin film composite membranes (TFC). Although this star-shaped acyl chloride has the same functionality as TMC, it is larger in size and its acyl chloride groups are less reactive due to the electron donating ether linkages. In this work, we prepared TFC membranes by the interfacial polymerization of both this star-shaped acyl chloride and TMC with either one of the two structural isomers: *m*-phenylenediamine (MPD) or *p*-phenylenediamine (PPD). No significant effect was observed of the substitution pattern of the aromatic diamine on the membrane formation with TMC, due to the high reactivity of the acyl chloride groups of TMC. In contrast, the use of this star-shaped acyl chloride results in significant differences in the properties of the formed TFC membrane depending on the use of MPD or PPD. Where TMC-MPD membranes are well-known for their excellent retention, we could not obtain defect-free membranes prepared from MPD and this star-shaped triacyl chloride ($R_{\text{rose bengal}}$<77%). The use of PPD instead of MPD, however, did result in defect-free membranes ($R_{\text{rose bengal}}$>97%) with an acceptable clean water permeance (2.5 L m^{-2} h^{-1} bar^{-1}).

Keywords: Interfacial polymerization, Polyamide, Monomer reactivity, Thin film composite

1. Introduction

Thin film composite (TFC) membranes are nowadays the industrial standard for, *e.g.*, reverse osmosis (RO). These TFC membranes consist of a thin dense top layer that is the actual separating layer, and a porous support that provides mechanical strength [1]. The first TFC membranes were developed by John Cadotte [2], who reported on a method to make these TFC membranes by interfacial polymerization (IP). Membranes prepared by IP showed to have a higher water flux and salt rejection as compared to membranes prepared by the Loeb-Sourirajan process. In a typical IP reaction, a bifunctional amine is dissolved into the aqueous phase, and a trifunctional acyl chloride is dissolved into

*Corresponding author. n.e.benes@utwente.nl

the organic phase [3]. These two monomers form a dense top layer at the interface of the two immiscible phases. The all-aromatic, highly cross-linked polyamide prepared from *m*-phenylenediamine (MPD) and trimesoyl chloride (TMC) [4], developed by John Cadotte, is used for the preparation of most commercial TFC membranes.

Alternative chemical structures to the commonly used MPD and TMC monomers have been published in literature [5]. All aim for improved membrane properties, such as enhanced permeability, salt rejection, stability, or fouling resistance. It was found that the substitution patterns of the aromatic rings of both the amine and the acyl chloride monomer have a strong effect on the rejection of the resulting membranes [6, 7]. For example, the performance of membranes prepared from either MPD or *p*-phenylenediamine (PPD) by the interfacial polymerization with TMC has been studied extensively [8–10]. It was found that TMC-MPD membranes have a more flexible chain structure as compared to TMC-PPD membranes [11], and hence have a higher water flux while retaining a similar salt rejection.

In addition to the trifunctional monomer TMC, membranes have been prepared from the bifunctional acyl chlorides isophthaloyl chloride (IPC) [6, 12, 13] or terephthaloyl chloride (TPC) [6]. The use of these bifunctional acyl chlorides reduces the amount of unreacted acyl chloride groups, but also reduces the degree of cross-linking when reacted with diamines. As compared to TMC-based membranes, the lower degree of cross-linking of IPC and TPC derived membranes results in a lower salt rejection [7, 14] and potentially in an increased swelling propensity. Therefore, one can claim that to be able to obtain highly cross-linked and stable top layers, the acyl chloride used should have a functionality of at least three.

A possible method to increase the acyl chloride functionality is to decorate a biphenyl with acyl chloride groups. A series of acyl chloride biphenyls with varying functionalities has been reported in literature by various authors. For example, the trifunctional 3,4',5-biphenyl triacyl chloride (BTRC) and the tetrafunctional 3,3',5,5'-biphenyl tetraacyl chloride (*mm*-BTEC) have been used in the preparation of TFC membranes [15]. These membranes were prepared from the interfacial polymerization of MPD with either BTRC or *mm*-BTEC. The performance of these membranes was compared to that of classical TMC-MPD membranes. BTRC-MPD membranes showed to have a higher cross-linking degree as compared to TMC-MPD membranes, resulting in a lower water permeance and higher salt rejection. Introducing the tetraacyl chloride *mm*-BTEC resulted in a further decrease of water permeance and increase in salt rejection. Further studies revealed that the use of BTEC structural isomers has a strong influence on the membrane performance. Membranes prepared from MPD and either *om*-BTEC or *op*-BTEC showed a significant increase in water permeance, while the rejection remained almost identical to *mm*-BTEC derived membranes [16].

In addition, membranes prepared from the pentafunctional biphenyl pentaacyl chloride [17] and the hexafunctional biphenyl hexaacyl chloride [18] have been reported in literature. The membranes prepared from these acyl chlorides with MPD follow the same trend as found for the tri- and tetrafunctional biphenyl acyl chlorides (Li et al.); a higher acyl chloride functionality lowers the water permeance. The salt rejection, however, was found to be independent on the acyl chloride functionality.

In summary, most structural variations to the commonly used TMC monomer, that are reported on in literature, are based on small rigid biphenyls with varying acyl chloride functionality ($3 \geq f \leq 6$). In this work, we did the opposite

and synthesized the larger and more flexible acyl chloride, 4,4',4"-[benzene-1,3,5-triyltris(oxy)]tribenzoyl chloride (**3**, Scheme 1), which has three acyl chloride groups. This acyl chloride has the same functionality as TMC, but is significantly larger. We expect that the use of such a large and flexible acyl chloride will have an effect on the free volume, the flexibility, and the morphology of the resulting TFC membranes. These TFC membranes were prepared by the interfacial polymerization of **3** with either MPD or PPD. The influence of this acyl chloride (**3**) and the diamine isomerism on the surface characteristics and membrane performance of the resulting membranes were compared to those of the commonly used TMC-MPD and TMC-PPD membranes.

2. Experimental

2.1. Materials

Phloroglucinol (≥99%), 4-fluorobenzonitrile (99%), thionyl chloride (≥98%), m-phenylenediamine (MPD, 99%), p-phenylenediamine (PPD,≥99%), and trimesoyl chloride (TMC, 98%) were obtained from Sigma-Aldrich (The Netherlands). Dried toluene was obtained from Merck (Germany) and Alfa Aesar (Germany). All chemicals and solvents were used as received.

*2.2. Synthesis of 4,4',4"-[benzene-1,3,5-triyltris(oxy)]tribenzoic acid (**2**)*

Compound **2** was synthesized from phloroglucinol and 4-fluorobenzonitrile, with compound **1** as intermediate, according to the procedure described by Matsumoto et al. [19]. ATR-FTIR (ν, cm^{-1}): 1675 (C=O), 1230, and 1004 (C−O−C). ^{1}H-NMR (DMSO, δ, ppm): 12.91 (s, 3H), 7.97 (d, 6H, J = 9 Hz), 7.17 (d, 6H, J = 9 Hz), 6.67 (s, 3H).

*2.3. Synthesis of 4,4',4"-[benzene-1,3,5-triyltris(oxy)]tribenzoyl chloride (**3**)*

Compound **2** (5.03 g, 0.01 mol) was dissolved in 40 mL of thionyl chloride under argon atmosphere. The mixture was heated to 80 °C and refluxed for 17 h. Excess thionyl chloride was removed by vacuum distillation, to yield an off-white powder (5.60 g, 100%). MP: 210 °C. ATR-FTIR (ν, cm^{-1}): 1740 (C=O), 1230, and 999 (C−O−C). ^{1}H-NMR ($CDCl_3$, δ, ppm): 8.13 (d, 6H, J = 9 Hz), 7.11 (d, 6H, J = 9 Hz), 6.66 (s, 3H). ^{13}C-NMR ($CDCl_3$, δ, ppm): 167, 162, 158, 134, 128, 118, 108, 50.

2.4. Synthesis of polyamide powders

Polyamide powders were prepared by vigorously stirring 20 mL of MPD or PPD (2 w/v% in H_2O, *i.e.*, 2 g in 100 mL) with 20 mL of acyl chloride (0.1 w/v% TMC or 0.2 w/v% **3** in toluene, *i.e.*, 0.1 or 0.2 g in 100 mL) for 15 minutes. The solids were filtered, washed with water and subsequently with acetone, and dried in a vacuum oven at 50 °C.

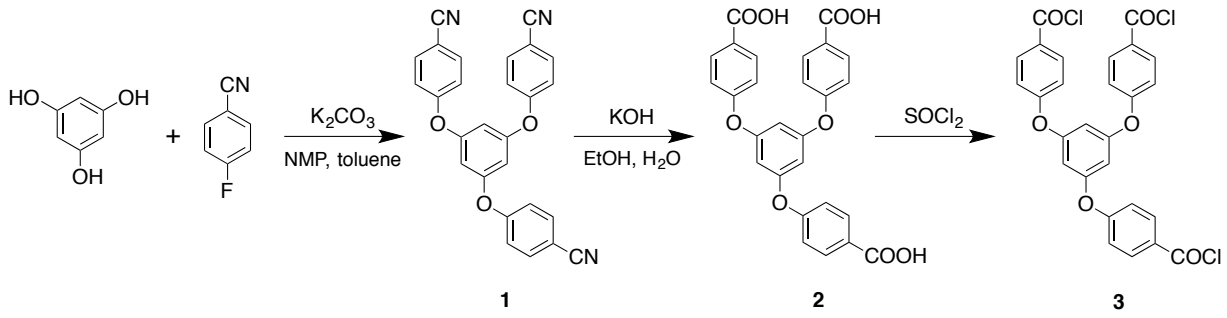

Scheme 1: Synthesis of the star-shaped trifunctional acyl chloride monomer 4,4',4"-[benzene-1,3,5-triyltris(oxy)]tribenzoyl chloride.

2.5. Preparation of polyamide films on silicon wafers

A silicon wafer (1.5×1.5 cm^2) was placed at the bottom of a petri dish (⌀2.5 cm). 5 mL of aqueous phase (2 w/v% amine) was poured into the petri dish. Subsequently, 3 mL of organic phase (acyl chloride in toluene) was poured on top of the aqueous phase. After 20 s both phases were removed with a pipette, while making sure that the forming freestanding film hit the surface of the wafer at 30 s. The film was carefully rinsed with water at least three times. The films were dried in a vacuum oven at 50 °C.

2.6. Synthesis of TFC membranes by interfacial polymerization

Thin film composite (TFC) membranes were prepared by the interfacial polymerization of **3** with either MPD or PPD on porous polyacrylonitrile (PAN) ultrafiltration supports (Solsep, the Netherlands). For comparison, membranes with TMC were prepared using a similar procedure. The structure of the polyamide obtained from the reaction of MPD or PPD with an acyl chloride is shown in Scheme 2. Because of the insufficient solubility of **3** in linear alkanes, such as *n*-hexane, toluene was chosen as organic phase. All TMC-based membranes were prepared with 0.1 w/v% TMC [20, 21]. The concentration of **3** was varied between 0.1–0.3 w/v%. The reaction time was kept constant at 30 s for all TFC membranes.

A typical procedure for the TFC preparation is given. The PAN support was clamped in a custom-built aluminum frame and 10 mL of aqueous solution (2 w/v% MPD or PPD in water) was poured into the frame atop of the PAN support, and the support was soaked for 5 minutes. The excess solution was drained off, and the frame was placed in a closed box which was flushed with nitrogen (<5% relative humidity). After 6 minutes of drying, the frame was removed from the box, and 10 mL of organic phase (0.1 w/v% TMC or 0.1–0.3 w/v% **3** in toluene) was carefully poured into the frame. After a reaction time of 30 seconds, the organic phase was removed and the TFC membrane was washed with toluene. The membrane was air-dried for 5 minutes, and stored in deionized water until use.

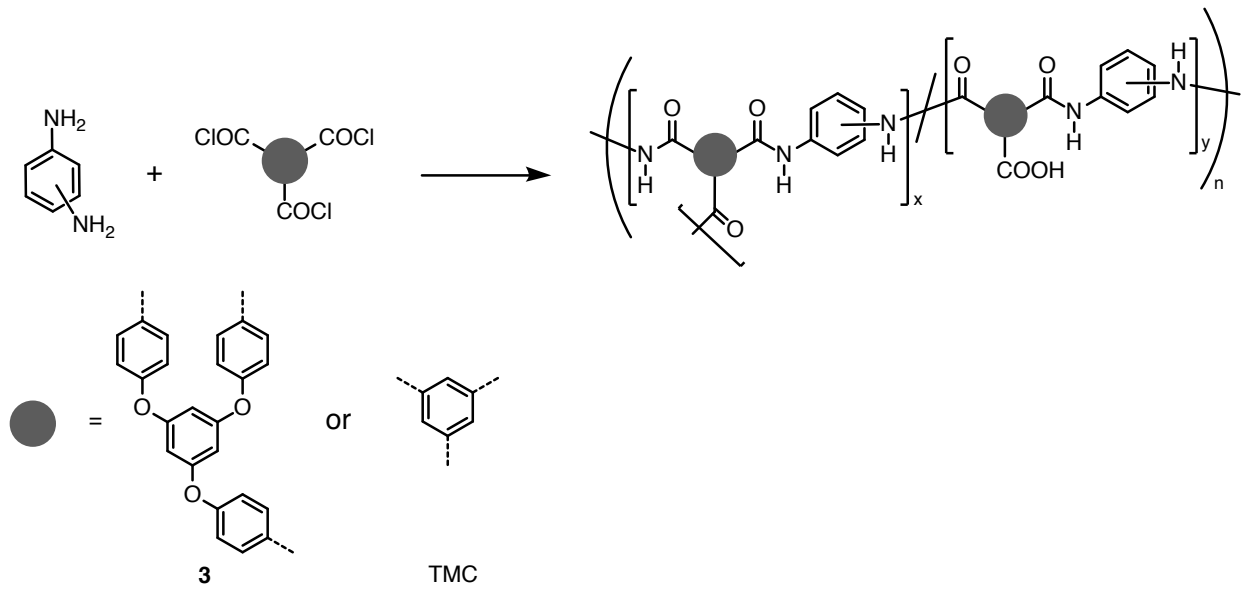

Scheme 2: The formation of a cross-linked network by the interfacial polymerization of a triacyl chloride (**3** or TMC) with MPD or PPD resulting in linear and cross-linked repeating units. The resulting polyamide networks contains carboxylic acid end-groups due to the hydrolysis of unreacted acyl chloride moieties.

2.7. Characterization

The chemical structures of the membranes were analyzed by Fourier transform infrared spectroscopy (FTIR) in attenuated total reflectance (ATR) mode on an ALPHA spectrometer (Bruker, Germany). Dried samples were pressed onto the diamond crystal without further sample preparation.

Thermal gravimetric analysis (TGA) measurements were performed with a Perkin Elmer TGA 4000 at 10 °C min^{-1} under nitrogen purge in aluminum pans. Combined thermogravimetric analysis (TGA) and mass spectroscopy (MS) measurements were performed using an STA 449 F3 Jupiter TGA with an alumina sample cup (Netzsch, Germany) and QMS 403 D Aeolos MS (Netzsch, Germany). The methods used for these combined TGA-MS measurements are described elsewhere [22]. Mass loss measurements were performed from 50 to 600 °C with a heating rate of 10 °C min^{-1} under a nitrogen atmosphere.

Scanning electron micrographs were taken with a JEOL JSM-7610 field emission scanning electron microscope (FE-SEM). Samples were coated with a 5 nm chromium layer (Quorum Q150T ES) prior to imaging.

Streaming current measurements were performed on a SurPASS analyzer (Anton Paar, Austria) equipped with an adjustable gap cell. The TFC membranes were fastened to the PDMS blocks (2 × 1 cm^2) of the cell with double sided adhesive tape. The pH of the electrolyte solution (5 mM KCl, $pH_{start} \approx 3.5$) was automatically adjusted using 0.1 M NaOH. The zeta potential of two different membranes was determined for each composition. From the streaming current, the zeta potential could be derived using Equation 1:

$$\zeta = \frac{\mathrm{d}I}{\mathrm{d}P} \cdot \frac{\eta}{\epsilon \cdot \epsilon_0} \cdot \frac{L}{A_{\mathrm{channel}}} \tag{1}$$

where: ζ is the zeta potential, $\frac{dI}{dP}$ is the slope of the streaming current versus pressure, η and ϵ are the viscosity and dielectric constant of the electrolyte, here taken as that of water, ϵ_0 is the permittivity of vacuum, L is the length of the streaming channel, and $A_{channel}$ is the cross sectional area of the channel.

The surface hydrophilicity of polyamide films deposited on silicon wafers was measured by static contact angle measurements using the sessile drop method (OCA 15, Dataphysics, Germany). Five separate water drops (1 μL) were deposited, and an image capturing the droplet was taken 3 s after the deposition.

The thickness of polyamide films deposited on silicon wafers was measured with an M2000X ellipsometer (J.A. Woollam Co., US) equipped with focusing probes. Spectra were recorded at three incident angles: 65°, 70°, and 75°. The film thickness was modelled (CompleteEase v4.86, J.A. Woollam Co., US) by a Cauchy layer atop of a silicon wafer bearing a 2 nm native oxide layer (fit parameters: A, B, k, and thickness).

Clean water fluxes were measured on a custom-built setup (Convergence, the Netherlands). All measurements were performed in cross-flow operation at a feed temperature of 25 °C with a membrane area of 46 cm^2. Permeate fluxes were measured using an M12 or M13 mini-Coriflow Coriolis mass-flow meter (Bronkhorst, the Netherlands).

Retention measurements were performed on a custom-built dead-end filtration setup. The membrane coupon (⌀39 mm), supported by a porous stainless steel disk, was mounted at the bottom of a stainless steel feed vessel. This vessel was pressurized to 15 bar with nitrogen gas. The feed was stirred with an overhead stirrer at 600 rpm to suppress concentration polarization. The first 20 mL of permeate was discarded from analysis.

The retention of two different solutes was determined: a 2000 pm aqueous NaCl solution and a 35 μM aqueous rose bengal solution (dye, 1017 g mol^{-1}). The concentration of the NaCl feed and permeate were analyzed by measuring the conductivity and temperature of the samples using a Cond 3310 conductivity meter (WTW, Germany). The concentration of the rose bengal feed and permeate was determined by measuring the UV-VIS absorbance of the samples at a wavelength of 549 nm (Shimadzu UV-1800 UV-spectrophotometer).

The retention R is defined as:

$$R = \frac{c_{feed} - c_{permeate}}{c_{feed}} \cdot 100\% \quad (2)$$

where c_{feed} is the concentration of the solute in the feed, and $c_{permeate}$ the concentration in the permeate. All retention experiments were carried out in dead-end mode. As a result, the concentration of the feed changes slightly over time. To compensate for this, the concentration of the solute in the feed was taken as the average of the original feed and the final retentate composition.

3. Results and discussion

3.1. Synthesis of the star-shaped trifunctional acyl chloride monomer

A star-shaped trifunctional acyl chloride monomer was prepared as outlined in Scheme 1. 4,4',4"-[Benzene-1,3,5-triyltris(oxy)]tribenzoyl chloride (**3**) was prepared from the reaction of phloroglucinol and 4-fluorobenzonitrile,

followed by hydrolysis and subsequent chlorination with thionyl chloride. The chemical analysis of compound **3** can be found in the supporting information.

3.2. Membrane synthesis and characterization

Polyamide TFC membranes have been prepared from a flexible acyl chloride and the aromatic diamines MPD and PPD. Scheme 2 shows the structure of this polyamide. ATR-FTIR spectra of the resulting TFC membranes prepared on PAN supports are given in Figure 1. All spectra are normalized to the PAN CN stretching at 2240 cm^{-1}. A strong amide I (C=O stretching) absorbance peak is present around 1661 cm^{-1} (Figure 1a) in the spectra of the TFC membranes prepared with TMC. Additionally, the TMC-MPD membrane shows a strong amide II (N–H bending) absorbance peak at 1537 cm^{-1}. The TMC-PPD membrane shows a shoulder at this position and a strong absorbance peak at 1513 cm^{-1}. Both TMC-MPD and TMC-PPD membranes show aromatic C=C stretching absorbance peaks at 1610 cm^{-1} and 1451 cm^{-1}.

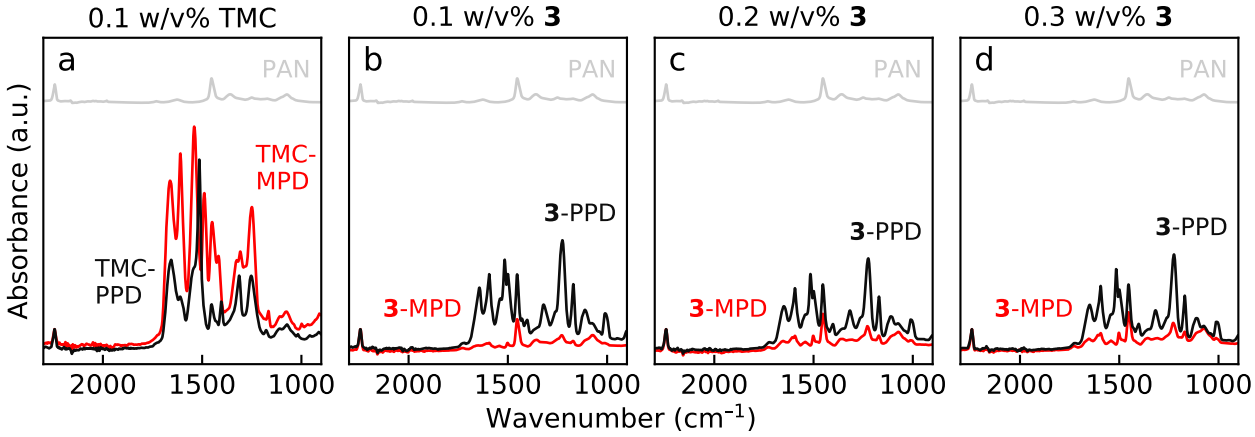

Figure 1: ATR-FTIR spectra of membranes prepared with (a) 0.1 w/v% TMC, (b) 0.1 w/v% **3**, (c) 0.2 w/v% **3**, and (d) 0.3 w/v% **3**. All membranes were prepared on porous PAN supports by applying a reaction time of 30 s. All spectra are normalized to the absorbance peak at 2240 cm^{-1}, originating from the CN stretching of PAN. The spectrum of the bare PAN support is given at the top as a reference (—). MPD-based membranes are represented in red (—), and PPD-based membranes in black (—). A peak originating from the C–O–C bond at 1000 cm^{-1} is only present in the **3**-based membranes.

The spectra of the **3**-based membranes prepared with various concentrations of **3** are shown in Figure 1b-d. While the ATR-FTIR spectrum of the acyl chloride **3** shows an absorbance peak due to the C=O stretching of the acyl chloride at 1740–1770 cm^{-1} (see supporting information), this peak has disappeared in the spectra of the **3**-based membranes. Instead, unreacted acyl chloride bonds hydrolyze towards carboxyl acids resulting in a small absorbance peak present at 1725 cm^{-1} belonging to the C=O stretch of the carboxylic acid.

3-PPD membranes show a strong amide I stretching around 1638 cm^{-1}, and the amide II bending around 1516 cm^{-1}, independent of the concentration **3** used. The aromatic C=C stretching is present at 1591 cm^{-1} and 1496 cm^{-1} for these membranes. An additional peak compared to the TMC-based membranes is present at 1009 cm^{-1}. This

peak originates from the C–O–C stretching of the ether linkage present in **3**. In contrast to the strong polyamide peaks present in TMC-MPD and **3**-PPD, **3**-MPD shows only very small polyamide peaks, and a small peak around 1008 cm^{-1} originating from the C–O–C stretching. The ratio of the polyamide to PAN peaks increases slightly with **3** concentration, but stays extremely small compared to the other polyamide membranes. This indicates that relative to the **3**-PPD membranes, there is not much **3**-MPD material present. This can be caused by either an extremely thin or a discontinuous top layer.

Unreacted acyl chloride groups present in the linear polyamide units hydrolyze into carboxylic acid groups upon contact with water. These carboxylic acid groups result in the negative surface charge which is common for polyamide membranes. Streaming current measurements were performed on all membranes, from which the zeta potential of the membrane's surface could be obtained (Figure 2). Figure 2a shows the zeta potential for TMC-based membranes and Figure 2b-d for **3**-based membranes prepared with 0.1, 0.2, and 0.3 w/v% acyl chloride, respectively.

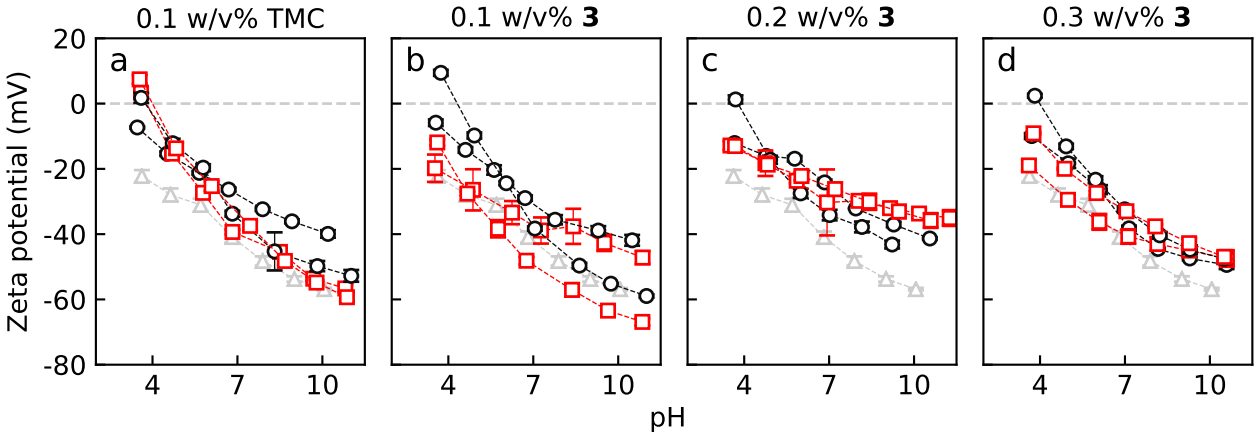

Figure 2: The zeta potential as function of pH of TFC membranes prepared with (a) 0.1 w/v% TMC, (b) 0.1 w/v% **3**, (c) 0.2 w/v% **3**, and (d) 0.3 w/v% **3**. All membranes were prepared on PAN supports by applying a 30 s reaction time. MPD-based polyamides are represented by red squares (□), and PPD-based polyamides by black circles (○). The zeta potential of a bare PAN support is added as a reference (grey triangles, △).

As expected, the TMC-based membranes show a negative surface charge over the whole pH range due to free carboxylic acid end-groups. In contrast to TMC, we expected that the use of the larger acyl chloride **3** would result in a reduction of the amide and carboxylic acid groups per unit of volume, and hence a more positively charged surface. However, from the zeta potential measurements, no significant increase in surface charge for the **3**-membranes as compared to the TMC-based membranes could be observed.

3.3. Membrane structure and morphology

The membrane structure and morphology were examined by top-view FE-SEM imaging. Figure 3 shows the results for the MPD-based membranes, and Figure 4 shows the results for the PPD-based membranes.

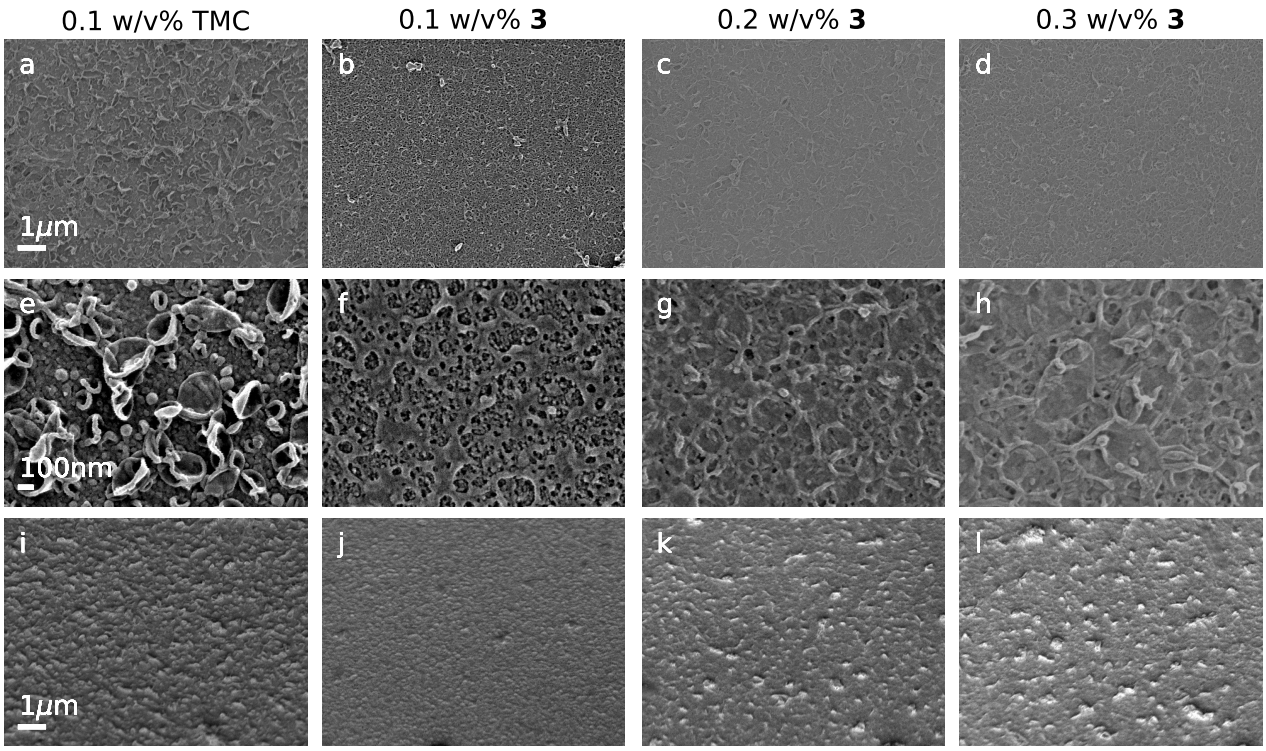

Figure 3: Top-view scanning electron micrographs of MPD-based membranes. (a-d) 10,000x magnification, (e-h) 50,000x magnification, and (i-l) 10,000x magnification with a stage angle of 45°.

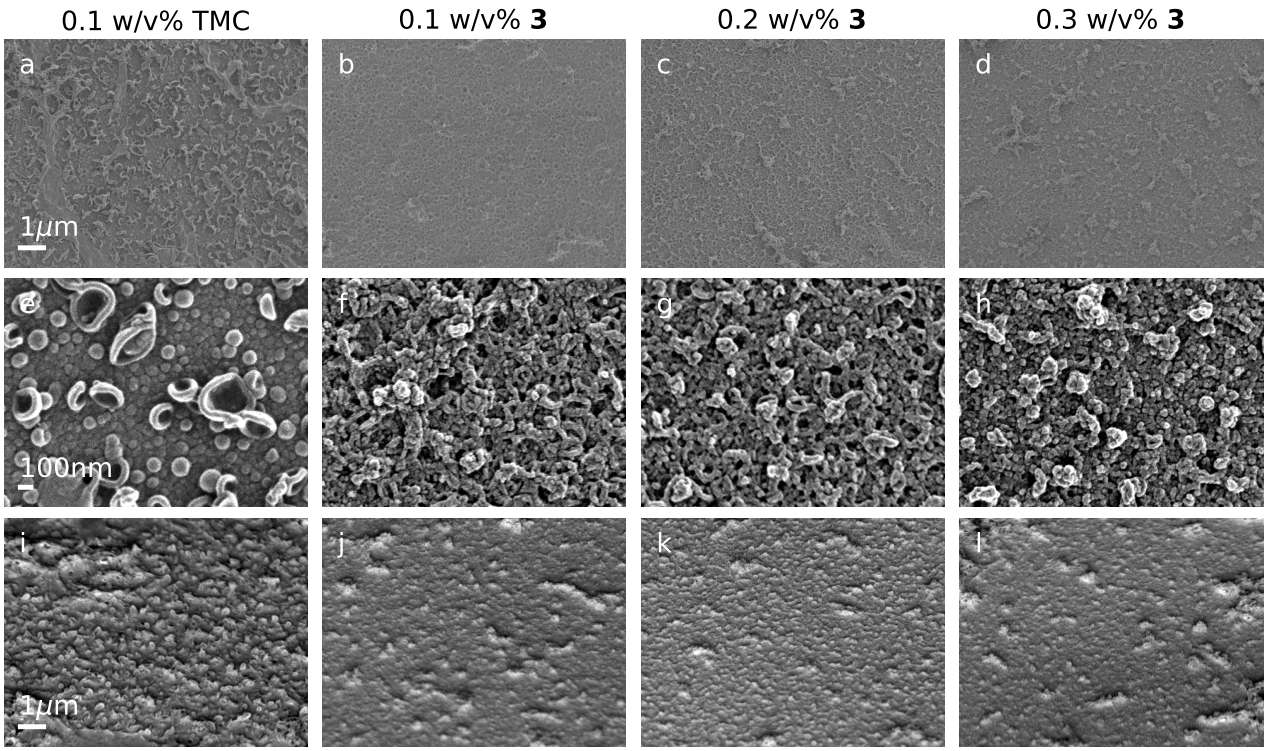

Figure 4: Top-view scanning electron micrographs of PPD-based membranes. (a-d) 10,000x magnification, (e-h) 50,000x magnification, and (i-l) 10,000x magnification with a stage angle of 45°.

The surface morphology of TMC-MPD and TMC-PPD membranes is frequently reported in literature. For example, Kwak et al. [9] reported FE-SEM micrographs for MPD-TMC and PPD-TMC membranes, respectively. The authors found a typical ridge-and-valley structure [23] with a tightly packed globular structure underneath for TMC-MPD membranes. In contrast, the surface morphology of TMC-PPD membranes looked more like a dense, finely dispersed nodular structure. Figure 3a,e shows a similar surface morphology of TMC-MPD membranes as to that reported by Kwak et al.. The TMC-MPD membranes have a nodular structure with ridge-and-valley features on top. The TMC-PPD membranes (Figure 4a,e) prepared in this study show a significantly reduction in the ridge-and-valley structure, whereas the nodular structure is clearly visible. These findings correspond relatively well to those reported by Kwak et al..

The substitution of TMC by compound **3** has a significant impact on the surface morphology of the polyamide formed. The nodular structure with ridge-and-valley features has disappeared. Instead, **3**-MPD membranes are found to have a polymer film-like structure that strongly depends on the concentration of acyl chloride. From Figure 3f, it can be clearly seen that 0.1 w/v% of **3** results in a very open polymer structure that only partially covers the PAN support (FE-SEM images of the PAN support can be found in the supporting information). Increasing the acyl chloride concentration to 0.2 or 0.3 w/v% results in a more densely packed polymer film that is still relatively smooth compared to the TMC-MPD membrane. The difference in surface roughness can be seen more clearly from Figure 3i-l where the sample stage was rotated at an angle of 45°.

The surface morphology of TMC-MPD and TMC-PPD membranes is similar. In contrast, the surface morphology of **3**-based membranes depends strongly on the isomerism of the diamine. The use of PPD results in a rough and grain-like surface morphology. In contrast to **3**-MPD membranes, no influence of the concentration of acyl chloride on the surface morphology of **3**-PPD membranes is observed.

3.4. The effect of chemical structure on the reactivity

From the FTIR and FE-SEM results it can be concluded that there is a significant difference in the reaction kinetics of the polyamide formation when either MPD or PPD is used in the interfacial polymerization with the acyl chloride **3**. The morphology of a membrane prepared by interfacial polymerization is greatly influenced by the diffusivity and solubility of the diamine monomer into the organic phase [24, 25]. However, we expect the diffusion rate and solubility of MPD and PPD to be similar, evidenced by the minor morphological differences found for TMC-based membranes. Therefore, we attribute this difference to a complex interplay of several factors.

First of all, the nucleophilicity of the amine groups differs slightly for MPD and PPD, as can be concluded from Table 1 that shows the resonance structures and pKa values for both MPD and PPD. The δ^- charges present in the aromatic ring of MPD reduce the nucleophilicity as compared to PPD that has a net zero charge in the aromatic ring. This difference in nucleophilicity is reflected in lower pKa values for MPD as compared to PPD.

Secondly, the formation of an amide bond influences the reactivity of the remaining amine group. An amide group is a moderately electron donating, and thus an activating, group. The δ^- charges present when one amine group has

Table 1: The resonance structure and pKa values of the diamines MPD and PPD.

Diamine	Structure	pKa_1 [26]	pKa_2 [26]
MPD	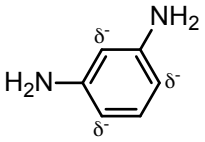	2.50	5.11
PPD	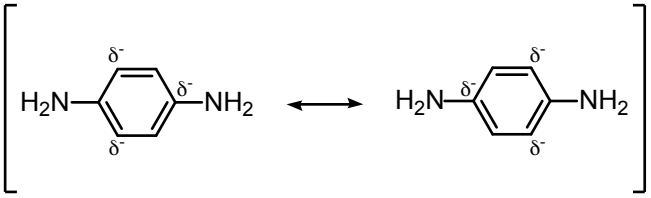	2.97	6.31

reacted towards an amide group are shown in Figure 5 for both *meta*- and *para*-substituted amides. The electron density of an *meta*-amide towards the amine group is unchanged compared to the diamine MPD. In contrast, the electron density towards the amine group is increased in an *para*-amide, and thus making this *para*-amide a better nucleophile.

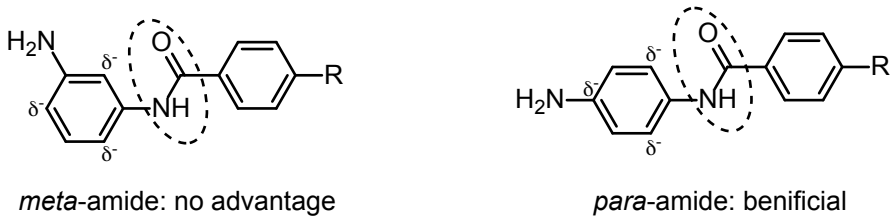

Figure 5: Formation of amide bonds will, depending on the substitution pattern of the aromatic diamine, enhance the reactivity of the amine group.

Thus, theoretically the use of a *meta*-substituted diamine reduces the reactivity and thus reaction rate. However, no significant difference in membrane performance is observed for TMC-based membranes prepared with either MPD or PPD. In addition, high performance linear polyamides with high molecular weights, such as Nomex®, Twaron®, and Kevlar® can be synthesized from both MPD and PPD [27]. Thus the (theoretically) slightly lower reactivity of MPD does not hamper the formation of these high molecular weight aramids.

Thirdly, the reactivity of the acyl groups of **3** is lower as compared to that of TMC due to the electron donating ether groups that render the acyl chloride groups of **3** less electrophilic. However, the polymerization of the bifunctional 4,4'-oxybis(benzoyl chloride) (COCl−Ph−O−Ph−COCl) with various aromatic diamines yields high molecular weight polyamides [28–30].

All these high performance polyamides are typically prepared in a single solvent. Interfacial polymerization, however, does not allow for control over the reaction stoichiometry at the interface since the concentration of monomers is

controlled by the diffusion of the diamine into the organic phase [31, 32]. The fast formation of a highly cross-linked makes it extremely difficult to study the reaction kinetics experimentally.

Lastly, the monomer **3** is more hydrophobic as compared to TMC, and since it is a larger monomer the amount of amide groups per unit of volume is reduced. This results in a lower ability to form hydrogen bonds per unit of volume, and thus in a lower swelling degree of the polymer. Additionally, the packing of the polymer chains has an influence on the properties of the polymer formed. In general, *meta*-amides are less densely packed as compared to *para*-amides [33]. Therefore, we hypothesize that the polymer **3**-MPD has the tendency to form a gel, whereas **3**-PPD precipitates more quickly into a well-defined cross-linked film due to enhanced chain packing.

3.5. Membrane performance

Table 2 shows the clean water permeance (CWP), NaCl retention, and rose bengal retention for all membranes prepared in this study. The CWP of **3**-based membranes is strongly dependent on the concentration of the acyl chloride, and more or less independent on the isomerism of the diamine. An acyl chloride concentration of 0.1 w/v% results in a very open top layer with a high CWP (50–65 L m^{-2} h^{-1} bar^{-1}. Increasing the acyl chloride concentration to 0.2 w/v% significantly reduces the CWP to the order of 4–10 L m^{-2} h^{-1} bar^{-1}. A further increase in acyl chloride concentration to 0.3 w/v% reduces the CWP further to 2–4 L m^{-2} h^{-1} bar^{-1}.

The NaCl and rose bengal retention follow the same trend as the CWP. However, membranes prepared with PPD are found to have a significantly higher NaCl retention as compared to membranes prepared with MPD. This fits well with our hypothesis that the monomer PPD can be considered to be more reactive compared to MPD. When comparing the retention to that of the classical TMC-MPD membranes, all **3**-based membranes show a very low NaCl retention. This is probably caused by the larger size of the **3** monomer, and thereby a larger d-spacing of the top layer.

The retention of rose bengal (1017 g mol^{-1}) can be considered as an indicator for a defect-free top layer. Again, higher retentions are obtained with higher concentration of acyl chloride, and retentions for PPD-based membranes are higher than those for MPD-based membranes. Membranes prepared with 0.3 w/v% **3** and 2 w/v% PPD have a defect-free top layer with a rose bengal retention of >97%.

Table 2: Membrane performance for membranes prepared with 2 w/v% amine and 30 s reaction time.

Membrane	c_{COCl}[a] (w/v%)	CWP[b] (L m^{-2} h^{-1} bar^{-1})		R_{NaCl}[c] (%)		$R_{rose\ bengal}$[d] (%)	
		Sample 1	Sample 2	Sample 1	Sample 2	Sample 1	Sample 2
TMC-MPD	0.1	5.0 ± 0.2	5.5 ± 0.3	93	88	99	99
3-MPD	0.1	64.9 ± 10.1	60.6 ± 3.6	1	0	7	8
3-MPD	0.2	4.4 ± 0.3	7.3 ± 0.4	1	3	44	69
3-MPD	0.3	2.0 ± 0.3	3.7 ± 0.6	3	9	73	77
TMC-PPD	0.1	2.0 ± 0.2	2.2 ± 0.1	38	30	[e]	[e]
3-PPD	0.1	49.8 ± 2.0	55.3 ± 2.6	0	0	24	39
3-PPD	0.2	8.3 ± 0.1	9.5 ± 0.3	5	6	95	89
3-PPD	0.3	2.4 ± 0.1	2.5 ± 0.1	24	16	98	97

[a] Concentration of acyl chloride in the organic phase.

[b] Clean water permeance with the 95% confidence interval that is calculated from the linear regression of the measured flux and transmembrane pressure. The flux was measured in cross-flow mode at a constant temperature of 25°C.

[c] Retention measured in dead-end mode at a transmembrane pressure of 15 bar with an aqueous 2000 ppm NaCl feed.

[d] Retention measured in dead-end mode at a transmembrane pressure of 15 bar with an aqueous 35 μM rose bengal feed.

[e] Not measured.

4. Conclusion

Here, we reported on the synthesis of a new star-shaped trifunctional acyl chloride that has been used in the interfacial polymerization with aromatic diamines to form polyamide TFC membranes. In contrast to TMC-based membranes, we found that the structural isomerism of the aromatic diamine has a great effect on the reaction kinetics, the surface morphology, and the membrane performance. Membranes prepared from **3**-MPD have a relatively smooth but discontinuous top layer, where **3**-PPD membranes have a grain-like surface morphology. Also the amount of polyamide material that is formed during the interfacial polymerization differs significantly. The conversion to **3**-PPD was in the order of TMC-based polyamides, however, the conversion to polyamide **3**-MPD was rather low. As a consequence, the *para*-amide **3**-PPD has superior membrane performance over the *meta*-amide **3**-MPD. Defect-free ($R_{rose\ bengal}$>97%) membranes were obtained with **3**-PPD. These membranes are found to have a clean water permeance of 2.5 L m^{-2} h^{-1} bar^{-1}, and a maximum NaCl retention of 24%. However, the performance of **3**-based membranes is much lower as compared to the conventionally used TMC-MPD membranes.

5. Acknowledgements

This work took place within the framework of the Institute for Sustainable Process Technology (ISPT, project BL-20-02) and within The Dutch Polymer Institute under project #718.

References

[1] I. J. Roh, A. R. Greenberg, V. P. Khare, Synthesis and characterization of interfacially polymerized polyamide thin films, Desalination 191 (2006) 279 – 290.

[2] D. Li, H. Wang, Recent developments in reverse osmosis desalination membranes, J. Mater. Chem. 20 (2010) 4551–4566.

[3] R. J. Petersen, Composite reverse osmosis and nanofiltration membranes, Journal of Membrane Science 83 (1993) 81 – 150.

[4] J. E. Cadotte, Interfacially synthesized reverse osmosis membrane, 1981. U.S. Patent 4 227 344.

[5] W. Lau, A. Ismail, N. Misdan, M. Kassim, A recent progress in thin film composite membrane: A review, Desalination 287 (2012) 190 – 199.

[6] I. J. Roh, S. Y. Park, J. J. Kim, C. K. Kim, Effects of the polyamide molecular structure on the performance of reverse osmosis membranes, Journal of Polymer Science Part B: Polymer Physics 36 (1998) 1821–1830.

[7] C. Kim, J. Kim, I. Roh, J. Kim, The changes of membrane performance with polyamide molecular structure in the reverse osmosis process, Journal of Membrane Science 165 (2000) 189 – 199.

[8] W. Choi, J.-E. Gu, S.-H. Park, S. Kim, J. Bang, K.-Y. Baek, B. Park, J. S. Lee, E. P. Chan, J.-H. Lee, Tailor-made polyamide membranes for water desalination, ACS Nano 9 (2015) 345–355. PMID: 25548959.

[9] S.-Y. Kwak, S. G. Jung, Y. S. Yoon, D. W. Ihm, Details of surface features in aromatic polyamide reverse osmosis membranes characterized by scanning electron and atomic force microscopy, Journal of Polymer Science Part B: Polymer Physics 37 (1999) 1429–1440.

[10] I. Juhn Roh, Effect of the physicochemical properties on the permeation performance in fully aromatic crosslinked polyamide thin films, Journal of Applied Polymer Science 87 (2003) 569–576.

[11] S.-Y. Kwak, Relationship of relaxation property to reverse osmosis permeability in aromatic polyamide thin-film-composite membranes, Polymer 40 (1999) 6361 – 6368.

[12] Y. Mo, A. Tiraferri, N. Y. Yip, A. Adout, X. Huang, M. Elimelech, Improved antifouling properties of polyamide nanofiltration membranes by reducing the density of surface carboxyl groups, Environmental Science & Technology 46 (2012) 13253–13261. PMID: 23205860.

[13] J. E. Cadotte, R. S. King, R. J. Majerle, R. J. Petersen, Interfacial synthesis in the preparation of reverse osmosis membranes, Journal of Macromolecular Science: Part A - Chemistry 15 (1981) 727–755.

[14] N. Saha, S. Joshi, Performance evaluation of thin film composite polyamide nanofiltration membrane with variation in monomer type, Journal of Membrane Science 342 (2009) 60 – 69.

[15] L. Li, S. Zhang, X. Zhang, G. Zheng, Polyamide thin film composite membranes prepared from 3,4',5-biphenyl triacyl chloride, 3,3',5,5'-biphenyl tetraacyl chloride and m-phenylenediamine, Journal of Membrane Science 289 (2007) 258 – 267.

[16] L. Li, S. Zhang, X. Zhang, G. Zheng, Polyamide thin film composite membranes prepared from isomeric biphenyl tetraacyl chloride and m-phenylenediamine, Journal of Membrane Science 315 (2008) 20 – 27.

[17] T. Wang, L. Dai, Q. Zhang, A. Li, S. Zhang, Effects of acyl chloride monomer functionality on the properties of polyamide reverse osmosis (ro) membrane, Journal of Membrane Science 440 (2013) 48 – 57.

[18] T. Wang, Y. Yang, J. Zheng, Q. Zhang, S. Zhang, A novel highly permeable positively charged nanofiltration membrane based on a nanoporous hyper-crosslinked polyamide barrier layer, Journal of Membrane Science 448 (2013) 180 – 189.

[19] K. Matsumoto, T. Higashihara, M. Ueda, Star-shaped sulfonated block copoly(ether ketone)s as proton exchange membranes, Macromolecules 41 (2008) 7560–7565.

[20] A. Ahmad, B. Ooi, Properties-performance of thin film composites membrane: study on trimesoyl chloride content and polymerization time, Journal of Membrane Science 255 (2005) 67 – 77.

[21] C. Klaysom, S. Hermans, A. Gahlaut, S. V. Craenenbroeck, I. F. Vankelecom, Polyamide/polyacrylonitrile (pa/pan) thin film composite osmosis membranes: Film optimization, characterization and performance evaluation, Journal of Membrane Science 445 (2013) 25 – 33.

[22] M. J. T. Raaijmakers, E. J. Kappert, A. Nijmeijer, N. E. Benes, Thermal imidization kinetics of ultrathin films of hybrid poly(poss-imide)s, Macromolecules 48 (2015) 3031–3039.

[23] J. Xu, H. Yan, Y. Zhang, G. Pan, Y. Liu, The morphology of fully-aromatic polyamide separation layer and its relationship with separation performance of tfc membranes, Journal of Membrane Science 541 (2017) 174 – 188.

[24] A. K. Ghosh, B.-H. Jeong, X. Huang, E. M. Hoek, Impacts of reaction and curing conditions on polyamide composite reverse osmosis membrane properties, Journal of Membrane Science 311 (2008) 34 – 45.

[25] B. Khorshidi, T. Thundat, B. A. Fleck, M. Sadrzadeh, A novel approach toward fabrication of high performance thin film composite polyamide membranes, Scientific Reports 6 (2016) 22069.

[26] J. R. Rumble (Ed.), CRC Handbook of Chemistry and Physics, CRC Press/Taylor & Francis, Internet version 2018.

[27] J. M. GarcÃŋa, F. C. GarcÃŋa, F. Serna, J. L. de la PeÃśa, High-performance aromatic polyamides, Progress in Polymer Science 35 (2010) 623 – 686.

[28] A. Abdolmaleki, S. HeshmatâĂŘAzad, M. KheradmandâĂŘfard, Noncoplanar rigidâĂŘrod aromatic polyhydrazides containing trÃűger's base, Journal of Applied Polymer Science 122 (2011) 282–288.

[29] M. Damaceanu, R. Rusu, A. Nicolescu, M. Bruma, Blue fluorescent polyamides containing naphthalene and oxadiazole rings, Journal of Polymer Science Part A: Polymer Chemistry 49 (2011) 893–906.

[30] M. Inoki, F. Akutsu, Synthesis and properties of polyamides and polyimides derived from diamines having 2-phenyl-4,5-oxazolediyl units and polyamide/montmorillonite composite, Journal of Macromolecular Science, Part A 48 (2011) 912–919.

[31] G.-Y. Chai, W. B. Krantz, Formation and characterization of polyamide membranes via interfacial polymerization, Journal of Membrane Science 93 (1994) 175 – 192.

[32] Y. Zhang, N. E. Benes, R. G. H. Lammertink, Visualization and characterization of interfacial polymerization layer formation, Lab Chip 15 (2015) 575–580.

[33] R. Ramani, T. Kotresh, R. I. Shekar, F. Sanal, U. Singh, R. Renjith, G. Amarendra, Positronium probes free volume to identify para- and meta-aramid fibers and correlation with mechanical strength, Polymer 135 (2018) 39 – 49.